CARBON letters

Note
Carbon Letters Vol. 23, 79-83 (2017)

Facile fabrication of electrospun polyacrylonitrile/poly(vinylidene fluoride)-based carbon nanofibers for supercapacitor electrodes

Hyo In Lee and Soo-Jin Park*

Department of Chemistry, Inha University, Incheon 22212, Korea

Article Info

Received 14 January 2017
Accepted 12 April 2017

***Corresponding Author**
E-mail: sjpark@inha.ac.kr
Tel: +82-32-876-7234

Open Access

DOI: http://dx.doi.org/10.5714/CL.2017.23.079

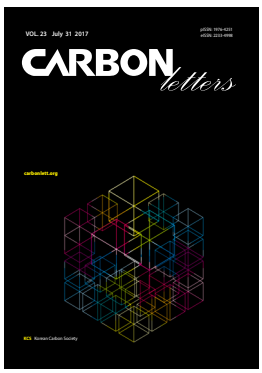

http://carbonlett.org

pISSN: 1976-4251
eISSN: 2233-4998

Energy storage devices and renewable energy sources are some of the most interesting alternatives being developed to solve the energy crisis [1,2]. At the same time, energy harvesting and storage devices are among the technologies with the highest potential to efficiently satisfy the energy requirements of compact electronic devices [3]. Among various energy storage devices, supercapacitors are the among the most intensely researched because of their high power density, long cycle retention, and rapid charge/discharge rates [4,5].

Depending on their particular charge/discharge mechanism, supercapacitors are classified into two categories: electrical double layer capacitors (EDLC) and pseudo-capacitors. EDLCs are charged by the electrostatic interaction between the electrode and electrolyte interfaces; i.e., EDLC electrodes use a mechanism involving the physical adsorption/desorption of electrolyte ions for the charging process. Generally, EDLC electrode materials include carbon materials with high surface areas, such as carbon black, graphene, carbon nanotubes, and carbon fibers [6,7].

The charging mechanism of pseudo-capacitors is based on reversible oxidation/reduction reactions (redox reactions). In operation, faradaic charge transfer reactions occur on the electro-active species of the electrode materials, which are typically transition metal oxides or conducting polymers [8,9]. Because the transition metals that are commonly used for pseudo-capacitor electrodes are prohibitively expensive for broad applications, alternatives such as carbon materials, which have low cost, are usually employed as the electrode materials [10].

Many attempts have been made to endow EDLCs with pseudo-capacitive properties to improve the specific capacitance of supercapacitors [11-13]. The introduction of heteroatoms into the carbon framework has been found to be a useful method. Specifically, the introduction of nitrogen species into the carbon matrix is known to induce additional pseudo-capacitance, and enhance the capacity, electronic conductivity, and surface wettability of the electrode materials while maintaining good cycle retention [14-16].

Polyacrylonitrile (PAN)-based carbon fibers are particularly interesting because acrylic fibers are high-performance engineered carbon fibers, which have a good carbonization yield [17,18]. Furthermore, PAN already has an internal nitrogen species which eliminates the need to separately introduce nitrogen into the carbon fibers. These characteristics provide a simple approach for preparing nitrogen-doped carbon fibers. Jo et al. investigated carbon fibers derived from various polymer blends; they reported that the PAN-based carbon fibers acquired a porous structure by blending with poly(vinylidene fluoride) (PVDF) without an activation process, because PVDF can generate a porous structure during the carbonization process [19-21].

In this study, we report the preparation of carbon nanofibers from an electrospun PAN/PVDF polymer blend followed by thermal carbonization treatments. The porous structure and nitrogen content of the prepared carbon nanofibers are controlled by the PAN/PVDF weight ratio, and the electrochemical performance was studied based on the porous and elemental properties.

N,N-dimethylformamide (DMF; ≥99.5%, Daejung Co., Korea), PAN (M_w 150,000; Sigma-Aldrich Co., USA), and PVDF (M_w ~534,000, Sigma-Aldrich Co.) were used for the

electrospun solution. PVDF and 1-methyl-2-pyrrolidone (NMP; ≥99.0%, TCI Co., Taiwan) were used to prepare the slurry for the electrochemical performance analyses. All chemicals were used without further purification.

A mixed PAN/PVDF polymer (10 wt%; PAN:PVDF (w/w)=100:0, 95:5, 90:10, 80:20, and 70:30) was dissolved in 25 mL of DMF and stirred for 12 h at room temperature. The prepared solution was placed in a 12 mL syringe and ejected from a stainless steel needle onto an aluminum foil-covered drum winder by an electrospinning apparatus (Nano NC, Korea). Electrospinning was performed with a supplied voltage of 15 kV, feeding rate of 0.8 mL h^{-1}, tip-to-collector distance of 15 cm, and collector speed of 300 rpm, which was achieved using a syringe pump (KDS-200; KD Scientific, USA). The temperature and relative humidity were kept at 25±2°C and 50±5%, respectively, during the spinning process. It is quite important to maintain constant atmospheric conditions because it can influence the properties of the prepared samples, such as porosity [22]. The electrospun mat-type polymer fibers were stabilized at 280°C for 1 h under air and were subsequently carbonized at 1000°C for 3 h under N_2 gas. The completed polymer-based carbon nanofibers (PCNFs) were labeled according to the PAN/PVDF weight ratio (e.g., PCNF-90/10). The synthesizing method is schematically illustrated in Fig. 1.

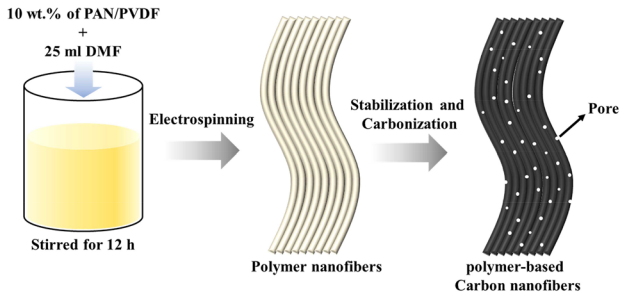

Fig. 1. A schematic description of the facile fabrication of the PAN/PVDF-based carbon nanofibers. PAN, polyacrylonitrile; PVDF, poly(vinylidene fluoride); DMF, N,N-dimethylformamide.

The morphology of the samples was observed by scanning electron microscopy (SEM; SU8010, Hitachi, Japan), and the pore structure was analyzed by N_2 adsorption/desorption isotherms. The isotherms were measured at liquid nitrogen temperature (77 K). The specific surface area and pore parameters, such as the pore size distribution and pore volume, were calculated by the Brunauer-Emmett-Teller equation and non-local density functional theory, respectively. Elemental analysis (EA; Thermo EA 1112, Thermo Fisher Scientific, USA) was performed to investigate the elementary composition of the prepared samples.

The electrochemical performance of the prepared materials, such as cyclic voltammetry (CV) and galvanostatic charge/discharge (GCD) tests, were conducted on an Iviumstat electrochemical workstation (Ivium Technologies, The Netherlands). All tests were performed using a three-electrode system: the PCNFs were used as the working electrodes, a platinum coil was used as the counter electrode, and a Ag/AgCl electrode was the reference electrode (in a 4.0 M KOH aqueous electrolyte). The slurry for the working electrode consisted of 80 wt% active materials (PCNFs), 10 wt% conductive materials (carbon black), 10 wt% binder (PVDF), and the solvent (NMP). The working electrode was prepared by loading the slurry onto nickel foam. CV was performed in the potential window of 0–0.4 V versus Ag/AgCl by varying the scan rate from 10 mV s^{-1} to 100 mV s^{-1}, and the GCD tests were performed at a current density of 5 A g^{-1} with a voltage range of 0–0.4 V versus Ag/AgCl.

SEM images show the morphology of the electrospun PCNFs (Fig. 2) and confirm the morphology change, from polymer powder to carbon nanofibers. The nanofiber diameters varied from 150 to 400 nm and decreased with increasing PVDF weight ratios. The mixed solutions for the electrospinning process had lower viscosities when the amount of PVDF was increased, which may lead to thinner carbon fibers [23]. However, there were no distinct differences observed in the surface roughness and shape [24].

Fig. 3a illustrates the N_2 adsorption/desorption isotherms of the PCNFs prepared with various weight ratios of PAN/

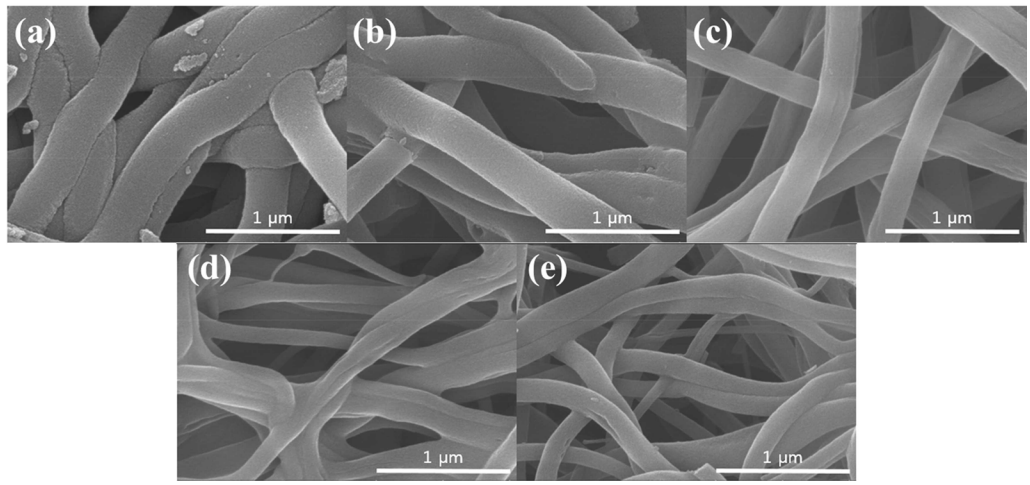

Fig. 2. Scanning electron microscopy images of the various prepared samples: (a) PCNF-100/0, (b) PCNF-95/5, (c) PCNF-90/10, (d) PCNF-80/20, and (e) PCNF-70/30. PCNF, polymer-based carbon nanofiber.

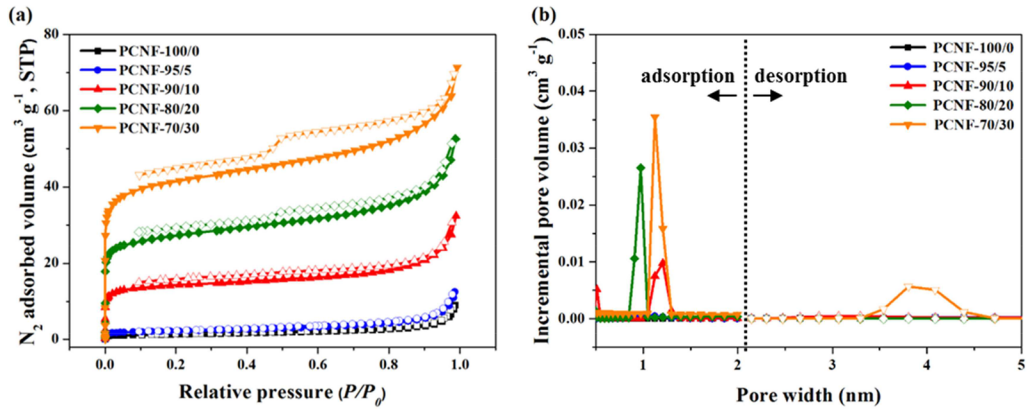

Fig. 3. (a) N_2 adsorption/desorption isotherms and (b) pore size distributions of the prepared samples. STP, standard temperature pressure; PCNF, polymer-based carbon nanofiber.

Table 1. The porous parameter and elemental analysis results of the PCNFs

Sample	S_{BET} ($m^2\ g^{-1}$)[a]	V_{total} ($cm^3\ g^{-1}$)[b]	V_{meso} ($cm^3\ g^{-1}$)[c]	V_{micro} ($cm^3\ g^{-1}$)[d]	D_p (nm)[e]	Elemental analysis (%, daf)			
						C	H	O[f]	N
PCNF-100/0	4	0.0172	0.00973	0.00137	12.45	79.40	0.61	12.16	7.80
PCNF-95/5	8	0.0461	0.0192	0.00262	9.77	81.28	0.59	11.37	7.22
PCNF-90/10	54	0.0944	0.0235	0.0262	3.70	84.19	0.51	8.26	7.01
PCNF-80/20	102	0.1249	0.0373	0.0513	3.20	85.36	0.51	8.59	5.52
PCNF-70/30	155	0.5414	0.0301	0.0704	2.82	87.62	0.59	8.49	3.27

PCNF, polymer-based carbon nanofiber; daf, dry ash free; NLDFT, non-local density functional theory.
[a] S_{BET}: specific surface area computed using Brunauer-Emmett-Teller equation at a relative pressure range of 0.00003–0.24.
[b] V_{total}: total pore volume is estimated at a relative pressure PP_0^{-1}=0.99.
[c] V_{meso}: mesopore (2–50 nm) volume determined from the NLDFT method.
[d] V_{micro}: micropore (0–2 nm) volume determined from the NLDFT method.
[e] D_p: average pore diameter.
[f] O: by difference.

PVDF. The isotherms are typical type I isotherms at low loading amounts of PVDF, while the isotherms of the PCNFs, which have high loading amounts of PVDF, present a type IV character (according to the International Union of Pure and Applied Chemistry [IUPAC] classification). The mesoporous structure of the PCNFs was determined by the presence of hysteresis loops [25,26]. The PCNF-80/20 and PCNF-70/30 desorption curves were separated, compared to the adsorption curves at low pressure. Loading the PVDF may generate internal pore structures in the PCNFs, and the pore structures could disturb the smooth desorption of N_2 molecules from the sample surfaces [20].

The pore size distribution obtained from the isotherms is presented in Fig. 3b and indicates that three of the samples have distinct microporous volume peaks (0–2 nm) and only one has a mesoporous volume peak (2–50 nm) [27,28].

The detailed pore structure parameters and EA results for the PCNFs are provided in Table 1. The specific surface area is found to be closely proportional to the weight ratio of the PVDFs, while the average pore diameter decreased with the increase in PVDF contents. Additionally, all of the samples had both microporous and mesoporous structures. The PAN/PVDF weight ratio influences the elemental composition of the PCNFs. As the PVDF percentage increases, the carbon content increases and the heteroatom content, such as oxygen and nitrogen, decreases.

CV measurements were performed to evaluate the electrochemical properties of the PCNFs. Fig. 4a shows the CV curves of the electrode loaded with PCNFs in a potential window of 0–0.4 V using a 4.0 M KOH aqueous solution as an electrolyte on the three-electrode system. The CV of the PCNFs displays a pair of strong cathodic/anodic peaks corresponding to the oxidation and reduction reaction (redox reaction), which indicates the contribution of double layer capacitance and pseudo-capacitance, which originates from the nitrogen content. From the CV curves, the specific capacitance can be obtained and directly proportioned to the areas of the CV curves,

$$C = \frac{1}{2m\Delta V}\int_{V_{initial}}^{V_{final}} \frac{|I|}{(dV/dt)}dV \quad (1)$$

where C is the specific capacitance; I is the instantaneous current at a given potential; $V_{initial}$ and V_{final} are the starting and ending potentials, respectively; m is the mass of the active materials,

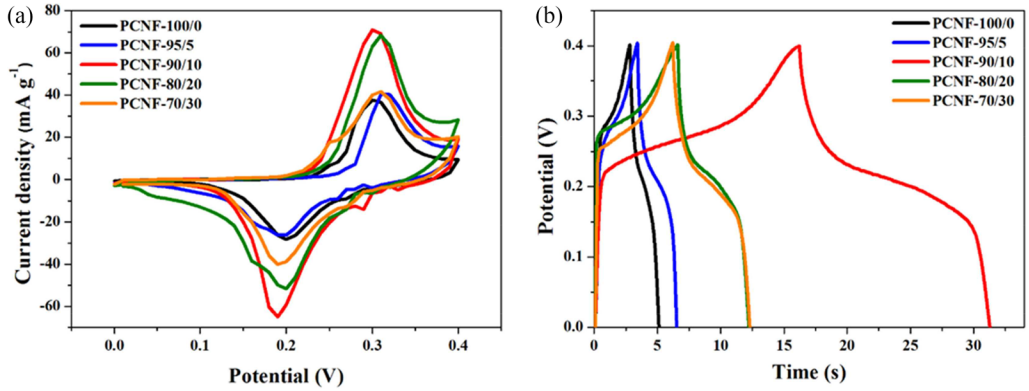

Fig. 4. (a) Cyclic voltammograms of the samples at a scan rate of 50 mV s^{-1} and (b) galvanostatic charge/discharge curves of the samples at a current of 5 A g^{-1}. PCNF, polymer-based carbon nanofiber.

and ΔV is the potential window for the CV measurements. The PCNF-90/10 exhibited the largest area of CV curves, implying the highest electrochemical performance.

To further investigate the performance of the PCNFs, GCD measurements were carried out at 5 A g^{-1} in a voltage range of 0–0.4 V (Fig. 4b). The GCD curves demonstrate the pseudo-capacitive character of the PCNF materials, which is distinguished by the triangular shape of the EDLCs. The specific capacitance can be obtained from the GCD measurements using the following equation,

$$C = \frac{I \times \Delta t}{m \times \Delta V} \quad (2)$$

where I is the applied current, Δt is the discharge time, and ΔV is the potential window for the GCD curves [29-31]. PCNF-90/10 showed the highest efficiency, in agreement with the CV results.

Among the samples, PCNF-70/30 had the largest specific surface area (its value was at least 100 m^2 g^{-1} greater than PCNF-90/10), but its specific capacitance was lower than that of PCNF-90/10. The results indicate that the nitrogen content significantly influences the specific capacitance [14]. The nitrogen content improves the wettability of the electrode surface and electrolyte by expanding hydrophilic polar sites. Furthermore, the nitrogen contents induce faradaic redox reactions leading to pseudo-capacitance. Such reactions enhance capacitance more strongly than physical adsorption/desorption reactions [32,33].

In summary, nitrogen-doped carbon nanofibers were simply synthesized in two steps: electrospinning and carbonization. Subsequently, the correlation between the precursor composition of the PAN/PVDF blends and their electrochemical performance were investigated. Blending different types of polymers increased the specific surface area of the carbon nanofibers, leading to enhanced electrochemical performances. However, PCNF-70/30 had the largest specific surface area and a lower efficiency than PCNF-90/10, which exhibited the highest electrochemical efficiency. The improvement in the performance of PCNF-90/10 was attributed to the nitrogen content of the samples, which allowed pseudo-capacitance following a redox reaction. The nitrogen content decreased with the addition of PVDFs, and a notable difference in the nitrogen content of PCNF-90/10 and PCNF-70/30 resulted in reduced electrochemical efficiency.

Conflict of Interest

No potential conflict of interest relevant to this article was reported.

Acknowledgements

This work was supported by a Inha University Research Grant.

References

[1] Huskinson B, Marshak MP, Suh C, Er S, Gerhardt MR, Galvin CJ, Chen X, Aspuru-Guzik A, Gordon RG, Aziz MJ. A metal-free organic-inorganic aqueous flow battery. Nature, **505**, 195 (2014). http://doi.org/10.1038/nature12909.

[2] Song R, Jin H, Li X, Fei L, Zhao Y, Huang H, Chan HLW, Wang Y, Chai Y. A rectification-free piezo-supercapacitor with a polyvinylidene fluoride separator and functionalized carbon cloth electrodes. J Mater Chem A, **3**, 14963 (2015). http://doi.org/10.1039/c5ta03349g.

[3] Cai X, Peng M, Yu X, Fu Y, Zou D. Flexible planar/fiber-architectured supercapacitors for wearable energy storage. J Mater Chem C, **2**, 1184 (2014). http://doi.org/10.1039/C3TC31706D.

[4] Hwang YH, Lee SM, Kim YJ, Kahng YH, Lee K. A new approach of structural and chemical modification on graphene electrodes for high-performance supercapacitors. Carbon, **100**, 7 (2016). http://doi.org/10.1016/j.carbon.2015.12.079.

[5] Amali AJ, Sun JK, Xu Q. From assembled metal-organic framework nanoparticles to hierarchically porous carbon for electrochemical energy storage. Chem Commun, **50**, 1519 (2014). http://doi.org/10.1039/C3CC48112C.

[6] Yu X, Kang Y, Park HS. Sulfur and phosphorus co-doping of hierarchically porous graphene aerogels for enhancing supercapacitor performance. Carbon, **101**, 49 (2016). http://doi.org/10.1016/j.carbon.2016.01.073.

[7] Li Y, Huang D, Shen W. Preparation of supercapacitors based on nanocomposites films of MnO_2/CB/C from sodium alginate

and MnO_2 nanoparticles by direct electrophoretic deposition and carbonization. Electrochim Acta, **182**, 104 (2015). http://doi.org/10.1016/j.electacta.2015.08.147.

[8] Zhai Y, Dou Y, Zhao D, Fulvio PF, Mayes RT, Dai S. Carbon materials for chemical capacitive energy storage. Adv Mater, **23**, 4828 (2011). http://doi.org/10.1002/adma.201100984.

[9] An GH, Koo BR, Ahn HJ. Activated mesoporous carbon nanofibers fabricated using water etching-assisted templating for high-performance electrochemical capacitors. Phys Chem Chem Phys, **18**, 6587 (2016). http://doi.org/10.1039/C6CP00035E.

[10] Miller JR, Simon P. Electrochemical capacitors for energy management. Science, **321**, 651 (2008). http://doi.org/10.1126/science.1158736.

[11] Huang L, Chen D, Ding Y, Feng S, Wang ZL, Liu M. Nickel–cobalt hydroxide nanosheets coated on $NiCo_2O_4$ nanowires grown on carbon fiber paper for high-performance pseudocapacitors. Nano Lett, **13**, 3135 (2013). http://doi.org/10.1021/nl401086t.

[12] Wang J, Liu S, Zhang X, Liu X, Liu X, Li N, Zhao J, Li Y. A high energy asymmetric supercapacitor based on flower-like $CoMoO_4$/MnO_2 heterostructures and activated carbon. Electrochim Acta, **213**, 663 (2016). http://doi.org/10.1016/j.electacta.2016.07.155.

[13] Liu Z, Nie H, Yang Z, Zhang J, Jin Z, Lu Y, Xiao Z, Huang S. Sulfur–nitrogen co-doped three-dimensional carbon foams with hierarchical pore structures as efficient metal-free electrocatalysts for oxygen reduction reactions. Nanoscale, **5**, 3283 (2013). http://doi.org/10.1039/C3NR34003A.

[14] Chen LF, Zhang XD, Liang HW, Kong M, Guan QF, Chen, P, Wu ZY, Yu SH. Synthesis of nitrogen-doped porous carbon nanofibers as an efficient electrode material for supercapacitors. ACS Nano, **6**, 7092 (2012). http://doi.org/10.1021/nn302147s.

[15] Si W, Zhou J, Zhang S, Li S, Xing W, Zhuo S. Tunable N-doped or dual N, S-doped activated hydrothermal carbons derived from human hair and glucose for supercapacitor applications. Electrochim Acta, **107**, 397 (2013). http://doi.org/10.1016/j.electacta.2013.06.065.

[16] Wu Y, Shi Q, Li Y, Lai Z, Yu H, Wang H, Peng F. Nitrogen-doped graphene-supported cobalt carbonitride@oxide core-shell nanoparticles as a non-noble metal electrocatalyst for an oxygen reduction reaction. J Mater Chem A, **3**, 1142 (2015). http://doi.org/10.1039/c4ta03850a.

[17] Beese AM, Papkov D, Li S, Dzenis Y, Espinosa HD. In situ transmission electron microscope tensile testing reveals structure–property relationships in carbon nanofibers. Carbon, **60**, 246 (2013). http://doi.org/10.1016/j.carbon.2013.04.018.

[18] Park SJ, Seo MK, Lee YS. Surface characteristics of fluorine-modified PAN-based carbon fibers. Carbon, **41**, 723 (2003). http://doi.org/10.1016/S0008-6223(02)00384-6.

[19] Abeykoon NC, Bonso JS, Ferraris JP. Supercapacitor performance of carbon nanofiber electrodes derived from immiscible PAN/PMMA polymer blends. RSC Adv, **5**, 19865 (2015). http://doi.org/10.1039/C4RA16594B.

[20] Yang Y, Centrone A, Chen L, Simeon F, Hatton TA, Rutledge GC. Highly porous electrospun polyvinylidene fluoride (PVDF)-based carbon fiber. Carbon, **49**, 3395 (2011). http://doi.org/10.1016/j.carbon.2011.04.015.

[21] Jo E, Yeo JG, Kim DK, Oh JS, Hong CK. Preparation of well−controlled porous carbon nanofiber materials by varying the compatibility of polymer blends. Polym Int, **63**, 1471 (2014). http://doi.org/10.1002/pi.4645.

[22] Megelski S, Stephens JS, Chase DB, Rabolt JF. Micro- and nanostructured surface morphology on electrospun polymer fibers. Macromolecules, **35**, 8456 (2002). http://doi.org/10.1021/ma020444a.

[23] Sutasinpromprae J, Jitjaicham S, Nithitanakul M, Meechaisue C, Supaphol P. Preparation and characterization of ultrafine electrospun polyacrylonitrile fibers and their subsequent pyrolysis to carbon fibers. Polym Int, **55**, 825 (2006). http://doi.org/10.1002/pi.2040.

[24] Seo MK, Park SJ. Electrochemical characteristics of activated carbon nanofiber electrodes for supercapacitors. Mater Sci Eng B, **164**, 106 (2009). http://doi.org/10.1016/j.mseb.2009.08.005.

[25] Yoon SH, Lim S, Song Y, Ota Y, Qiao W, Tanaka A, Mochida I. KOH activation of carbon nanofibers. Carbon, **42**, 1723 (2004). http://doi.org/10.1016/j.carbon.2004.03.006.

[26] Tang K, Li Y, Cao H, Su C, Zhang Z, Zhang Y. Amorphous-crystalline TiO_2/carbon nanofibers composite electrode by one-step electrospinning for symmetric supercapacitor. Electrochim Acta, **190**, 678 (2016). http://doi.org/10.1016/j.electacta.2015.12.209.

[27] Ra EJ, Raymundo-Piñero E, Lee YH, Béguin F. High power supercapacitors using polyacrylonitrile-based carbon nanofiber paper. Carbon, **47**, 2984 (2009). http://doi.org/10.1016/j.carbon.2009.06.051.

[28] Im JS, Park SJ, Kim TJ, Kim YH, Lee YS. The study of controlling pore size on electrospun carbon nanofibers for hydrogen adsorption. J Colloid Interface Sci, **318**, 42 (2008). http://doi.org/10.1016/j.jcis.2007.10.024.

[29] Liu X, Du G, Zhu J, Zeng Z, Zhu X. NiO/$LaNiO_3$ film electrode with binder-free for high performance supercapacitor. Appl Surf Sci, **384**, 92 (2016). http://doi.org/10.1016/j.apsusc.2016.05.005.

[30] Sinprachim T, Phumying S, Maensiri S. Electrochemical energy storage performance of electrospun AgO_x-MnO_x/CNF composites. J Alloys Compd, **677**, 1 (2016). http://doi.org/10.1016/j.jallcom.2016.03.174.

[31] Xie Q, Zhou S, Zheng A, Xie C, Yin C, Wu S, Zhang Y, Zhao P. Sandwich-like nitrogen-enriched porous carbon/graphene composites as electrodes for aqueous symmetric supercapacitors with high energy density. Electrochim Acta, **189**, 22 (2016). http://doi.org/10.1016/j.electacta.2015.12.087.

[32] Lota G, Grzyb B, Machnikowska H, Machnikowski J, Frackowiak E. Effect of nitrogen in carbon electrode on the supercapacitor performance. Chem Phys Lett, **404**, 53 (2005). http://doi.org/10.1016/j.cplett.2005.01.074.

[33] Hulicova−Jurcakova D, Seredych M, Lu GQ, Bandosz TJ. Combined effect of nitrogen− and oxygen−containing functional groups of microporous activated carbon on its electrochemical performance in supercapacitors. Adv Funct Mater, **19**, 438 (2009). http://doi.org/10.1002/adfm.200801236.